Electrical Properties of Solvated Tectomers: Towards Zettascale Computing

Alessandro Chiolerio[a], Thomas C. Draper[b], Carsten Jost[c], Andrew Adamatzky[b]

[a]*Istituto Italiano di Tecnologia, Center for Sustainable Future Technologies,*
Via Livorno 60, 10144 Torino, Italy
[b]*Unconventional Computing Laboratory, University of the West of England,*
Coldharbour Lane, Bristol, BS16 1QY, UK
[c]*PlasmaChem, Schwarzschildstr. 10, D-12489, Berlin, Germany*

Abstract

Liquid cybernetic systems with embodied intelligence solutions mimicking biologic systems, in response to the future increasingly distributed sensing and the resulting data to be managed, has been proposed as the next cybernetic paradigm. Storing and computing information inherently pushes research towards extremely high packing densities, shifting from classical into quantum (particle, molecular) physics, chemistry and materials science with the drawback of requiring very expensive equipment and exotic matter or matter states. Solutions represent a cheap and easy-to-handle platform for data storage and readout *in liquido*, where a physical structure able to change configuration under electrical stimuli reversibly exchanges entropy with the external environment. We propose tectomers as a candidate for such an adaptive structure. A tectomer is an oligomer made of few oligoglycine units with a common centre. Tectomers undergo pH dependent assembly to form a single layer supramer across a surface. Tectomers represent a stable paradigm, in their amorphous or crystalline forms, reversibly influenced by solution pH, whose electronic properties are studied herein. We will see, through a reasonable hypothesis, how solvated cybernetic systems could be exploited in the rush for zettascale computing.

Keywords: tectomer, oligoglycine, self-assembly, supramolecular, electrochemistry, ZFlop

In memory of Dr Alexey Kalachev, founder of PlasmaChem.

1. Introduction

Liquid robotics, in response to the future increasingly distributed sensing and the resulting data to be managed, has been proposed as the next cybernetic paradigm [1]. Envisaged solutions require the development of energy management subsystems [2], mobility subsystems, liquid state sensors, and liquid state logic devices and memories [3, 4], most importantly.

Several species of liquid robots have been proposed so far. Chemotactic droplet robots move along gradients of Marangoni flow [5]. Hardware robots can be equipped with liquid brains [6], thus only actuators and interface are conventional. Robots based on electro-rheological fluids propel due to sol-gel phase transitions [7]. Oil micro-droplets move in a cationic surfactant solution [8]. Swimming wet & soft robots are made of ionic polymer metal composites [9, 10]. Liquid metal robots that swim have been demonstrated, exploiting the interaction of Galinstan with aluminium and the resultant imbalance of surface tension induced by the bipolar electro-chemical reaction [11, 12]. All existing prototypes of liquid robots move either along chemical, thermal, electrostatic, magnetostatic or electro-magnetic gradients or due to geometrical constraining of space. Their environment is pre-programmed. To enable the liquid robots with an ability to make a choice we must equip them with a liquid or colloidal brain. Purely liquid controllers, being a subset of liquid computers [13], can be implemented as (micro-)fluidic logical circuits or reaction-diffusion media. Fluidic devices are realized on elaborate geometrical constraining, while reaction-diffusion controllers are slow and have a short lifetime [14].

Another way to implement computing and memory devices in the liquid phase is to select biochemical species which undergo controllable assembly and disassembly. Their intrinsic parallelism, due to the presence of a number of elementary processing units (the molecules or monomers dispersed in a solvent), suggests that a liquid state logic device could be used with non-conventional architectures, such as Holonomic ones [15]. Solutions for data storage and readout *in liquido* require a physical support able to change configuration under either electrical or optical stimuli (or both).

We propose that data storage can be implemented with tectomers, as well as computation. A reasonable set of arguments will be articulated to support the hypothesis that liquid cybernetic systems are suitable for implementing zettascale computing (10^{21} operations/s); a milestone which is expected to be reached in 2035 [16].

A tectomer is an oligoglycine molecule comprised of multiple repeating glycine units linked to a common hydrocarbon centre (Fig. 1a–c) [18, 19]. The 'tails' of a tectomer are not linear, but instead form a helical structure. These helical oligoglycines form polyglycine II-type structures, stabilized by hydrogen bonds in three directions [20]. The stabilizing intermolecular hydrogen bonds between the tectomers is facilitated by the glycine units, and therefore the longer the repeating chain, the more stable the resulting supramer. Tectomers are known to assemble into stable and rigid regular layers of mono-molecular thickness (Fig. 1d) [18, 17]. As demonstrated in [21], the positively charged structures with high electrophoretic mobility are formed up to 30th minute after preparation of the solutions. The sizes of tectomers and their electrical charges remain preserved for at least 24 hours. Whilst these supramer-forming tectomers are relatively new to the research community, there have already been suggestions that they may have antiviral properties [18, 17].

Two-dimensional platelets of tectomers have been previously incorporated into one-dimensional nanowire networks of silver nanowires, and transparent
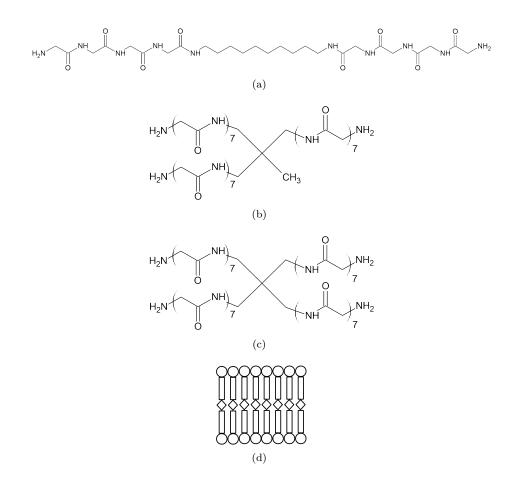
2

(a)

(b)

(c)

(d)

Figure 1: Tectomers. Chemical structure of (a) 2-tailed (T2), (b) 3-tailed (T3), and (c) 4-tailed (T4) tectomers. (d) Supramer. ◇ is $-(CH_2)_n-$, rectangle is olygoglycine tail, and ○ is an amino group. The scheme is redrawn from [17].

electrodes were obtained [22]. The tectomers brought several advantages: increased conductivity of the network by strengthening contacts between nanowires, protected silver nanowires against oxidation and sulfurization, and prevention of detachment of nanowires in case of immersion in aqueous medium [22].

The assembly of tectomers is pH dependent. Increase of pH leads to aggregation and assembly into ordered (crystalline) structures; while decrease of the pH causes dissolution and amorphous structures [23]. Therefore the stable aggregation state and the self-assembly capability of tectomers could be exploited to realize a pH-stabilized system with electrical read-out. In the following section 2, details about our experimental setup are given; while in section 3, details about electronic properties characterization are presented.

3

2. Methods and Materials

Lyophilised 2-, 3- and 4-tailed tectomers were supplied by PlasmaChem (Berlin, Germany), potassium phosphate monobasic was provided by Sigma Aldrich, and sodium hydroxide was provided by Fisher Scientific. All chemicals were used without further purification. Throughout this text 2-, 3- and 4-tailed tectomers are denoted as T2, T3 and T4 respectively. To prepare a solution of tectomers, 1.0 mg of the desired tectomer was dissolved in 1.00 mL of either deionized water (DIW, 15 MΩ cm) or a buffered aqueous solution. This provided concentrations for T2, T3, and T4 of 1.59 mM, 0.76 mM, and 0.58 mM, respectively. To aid dissolution, samples were subjected to an ultrasonic bath (Ultrawave U300H, 35 W, 30 kHz) for 15 minutes. Aqueous buffer solutions with a pH of 5.9 and 8.2 were both prepared using DIW, KH_2PO_4 (0.10 M) and adjusted using NaOH. The pH was measured using a calibrated Perkin Elmer P200-02 pH Meter. All experiments were performed using 10.0 µL droplets, and were unstirred thus allowing for diffusion-control.

Electrical stimulation and recording was performed via needle electrodes with twisted cables (Spes Medica Srl, Italy). These electrodes were inserted 1 mm deep into the tectomer solution droplet, and the distance between them kept at 2 mm. Fresh electrodes were used between each droplet, to prevent the effects of droplet evaporation and tectomer coating of the electrodes. The electronic characterization was assessed using a Keithley SCS4200 with triaxial cables and preamplifiers. DC characterisation was conducted in the range [-1.2, +1.2] V, with a step size of 20 mV, recording always 10 cycles and computing averages using 6 out of them. The voltage limit was chosen to avoid the electrolysis of water at 1.23 V. AC measurements have been taken in the range from 1 kHz to 10 MHz, typically with a signal amplitude of 10 mV RMS. By adding a DC bias and sweeping it between two saturation values (-0.5 V and +0.5 V), impedance is measured at a fixed frequency with a small signal over-imposed (10 mV RMS). Pulse Train (PT) measurements feature a high speed pulse generator with internal reference and feedback system that is capable of measuring its own output, plus two independent high speed voltage and current units connected to the device. By simultaneously monitoring the voltage and current at each of the electrodes, the real resistive response is measured under the application of multiple unipolar pulses. The pulse is rectangular, has an amplitude of 0.5 V and a duration of 1 ms, selected to be comparable to biologic action potentials. The electrical response is recorded for further 200 µs, enabling us to trace the decay of the sample to rest condition (0 V). During each measure the sample is submitted to a train of 50 pulses separated by 4 ms idle time and the resistive response is recorded and internally averaged; this procedure is repeated 10 times to trace any eventual drift and averaged to compute standard deviation.

4

3. Results

3.1. DC measurements

DC properties of the different tectomers in DIW and at different pH have been assessed. Figure 2(a) shows the average current-voltage (I-V) cycle measured by testing pure DIW, in a range of 1.2 V, as well as the two buffer solutions having a pH of 5.9 and 8.2 respectively. No higher potentials were produced to avoid water decomposition and related electrical instability. The cycle shows a relevant hysteresis, due to the droplet associated parasitic capacitance, and a maximum current of about 70 nA flowing through the DIW sample; the buffer solutions allow a current close to 800 nA, as expected from the increased ionic force. Quadrants are referred to by numbered convention, starting with quadrant I in the top right, proceeding anti-clockwise, and ending with quadrant IV in the bottom right.
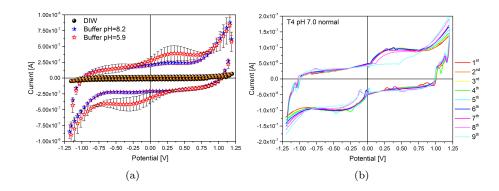

Figure 2: I-V cycle: (a) I-V curve of DIW, and the two buffers (pH = 8.2, 5.9). (b) T4 pH = 7.0, nine cycles of I-V.

For comparison, Fig 2(b) shows the response of a T4 sample at neutral pH, the first nine cycles are plotted. During measurements the sample appears to re-configure the order of molecules, so that the maximum current flowing is increased from about 120 nA in the first cycle to about 180 nA in the last. This is in addition to the diffusion-controlled hysteresis typically observed when conducting a non-stirred cyclic voltammetry experiment, due to the local depletion of reactive species at the electrodes and the consequential reliance on the rate-limited diffusion of molecules under the effects of an electric field [24, 25]. There is a small element of quasi-reversibility to the later runs, which is likely due to the tectomer beginning to adsorb onto the surface of the electrodes [17]. Furthermore the shape of the curve, though retaining qualitatively the features seen with DIW, reveals other phenomena.

The three tectomers have rather different responses. In Fig. 3(a) their average ($n = 10$) I-V curves have been compared, under pH 7.0. The cycles opens more for T2 and T3, while T4 features points with negative differential resistance both in quadrant I and III as well as second order discontinuities across the zero
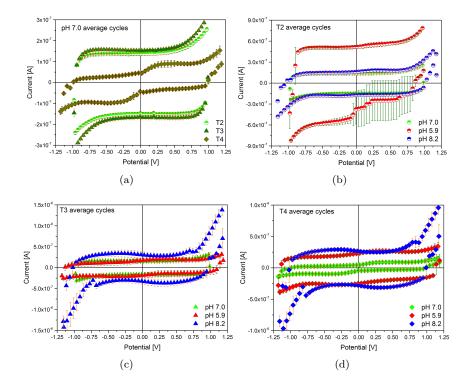
Figure 3: (a) Comparison between T2, T3 and T4 at pH=7.0. (b) T2, comparison between pH=5.9, 7.0 and 8.2. (c) T3, comparison between pH=5.9, 7.0 and 8.2. (d) T4, comparison between pH=5.9, 7.0 and 8.2. All graphs are the average of 10 runs, and only 1 point in every 10 is shown for clarity.

potential point. The standard deviation is very low for all the three samples, confirming their stability. Maximum current is about 300 nA for T3 sample. Figure 3(b) shows a comparison between responses of T2 tectomers in three different pH conditions, basic (pH 8.2), neutral (pH 7.0) and acidic (pH 5.9). While the basic and neutral solutions have very similar responses, the acidic condition produces a much more conductive state (approximately three times the others) with an unstable region in quadrant IV where a resistive switching occurs, with a set voltage found in the range (-40 mV, +880 mV). Figure 3(c) shows the same comparison as above for the T3 molecule. This suggests the application as resistive switching device (RSD), having a unipolar switching (switching occurs only in one portion of the hysteresis loop, here for positive potentials). In this case, the acid and neutral conditions have a very similar response, while the basic solution achieves much higher currents (up to 1.5 μA) and features in every quadrant negative differential resistance. Figure 3(d) shows the comparison for the T4 molecule, similar to the case of T3. Here the basic solution has negative differential resistance in quadrant IV.

In the case of the acidic T2 sample, it is likely that the pH has been reduced sufficiently for protonation of one of the terminal primary amine groups. As such the resulting solution would be more conductive due to the increase in the ionic mobility of T2. Equally, T3 appears to become (at least partially) deprotonated at a pH of 8.2, but not protonated at a pH of 5.9. Finally the T4 sample, having a higher current at both elevated and diminished pH levels, would appear to be able to undergo both protonation and deprotonation in the respective environments.

3.2. AC measurements

Due to connector parasitic impedance it is difficult to measure high impedance materials, therefore as a reference in every plot the curve of DIW and the buffer solutions has been shown for comparison (Fig. 4), to help reveal that the measurements are significant. Each curve reports also standard deviation, indicating that the noise level is higher in the range of 1 kHz to 10 kHz. Typically the samples kept at neutral pH show a higher resistance and a very similar response, while both the samples kept in basic and acid pH show a negative resistance range up to 100 kHz as well as some differences between T2, T3 and T4. The reactance of neutral samples shows the fingerprints of peaks found in DIW response (from 1 kHz to 10 kHz). Typically reactance is higher for neutral samples and the smallest for the basic sample; it decreases with frequency, as for predominantly capacitive materials. The only sample with a clear inductive behaviour is T4 in the neutral state, showing a negative reactance in the low frequency region of the spectrum. Generally speaking, our measures demonstrate that it is possible to distinguish between the different tectomers by measuring their impedance in the range between 1 kHz and 1 MHz, and that solvated tectomers absorb energy in the explored range of frequencies, since the pure buffer solutions have a much smaller impedance.
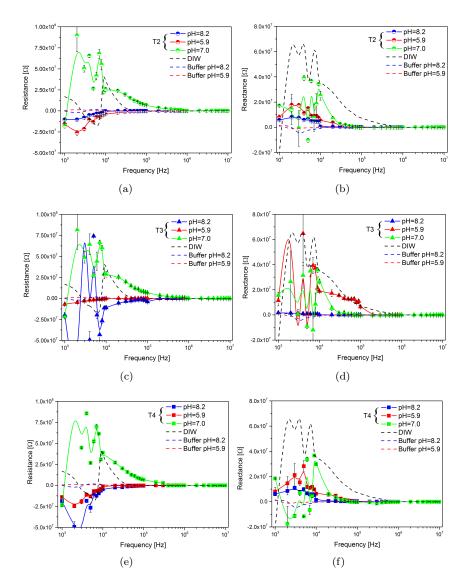
7

Figure 4: Impedance measurements in the range between 1 kHz and 10 MHz, for all tectomer sample T2 (a,b), T3 (c,d) and T4 (e,f) in all pH states and for DIW and the two buffer solutions. Average curves out of multiple measurements, standard deviation also shown.
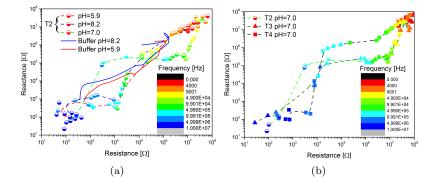
8

Figure 5: Nyquist plot for (a) sample T2 in three pH conditions, compared to the pure buffer solutions, and (b) samples T2, T3 and T4 in the neutral state. Both resistance and reactance shown in logarithmic scale after taking absolute value.

3.2.1. Frequency response

As alternative view, the Nyquist plot includes both the real and imaginary components of impedance (absolute value) on the same plane and shows frequency as a colour scale. In Fig. 5(a) the impedance of sample T2 is shown under the three pH values; increasing the signal frequency, reading the plot from top right to low left, both real and imaginary components are reduced. The non-neutral solutions retain a lower impedance with respect to the neutral one in the low frequency range of spectrum, until 50 kHz, in reason of their higher ion contribution to conductivity. Interestingly the reactance of the neutral sample is almost constant from 50 kHz up to about 1 MHz, making it very easy to discriminate between neutral and non-neutral conditions. Furthermore, comparing those plots with the pure buffers, we can see how different the fingerprints are. Figure 5(b) compares the Nyquist plots of the three tectomers in their neutral state. T2 and T3 show a very similar response up to 1 MHz, including the reactance stability plateau. T4 has a similar curve, the reduction of impedance vs frequency featuring a more gentle slope and a stability plateau, in a similar frequency range, placed at higher reactance values. Therefore the range between 100 kHz and 1 MHz can be used to discriminate between different tectomers.

3.2.2. Bias response

Building on top of AC stimulus a DC bias, no variation is seen at 1 kHz and 100 kHz (impedance is not a function of DC bias), while interesting features appear when samples are characterized at 10 MHz. This applies to all the pH conditions, producing patterns of different shape. Results are shown in Fig. 6, a 3D graph where DC bias, series resistance and capacitance represent the three axes (fixed frequency and fixed signal amplitude), while the colour code identifies different measurement sets. Taking T2 as example, the bias acts on impedance by reducing resistance and increasing capacitance by one quarter of its absolute value, moving from negative to positive potentials. More
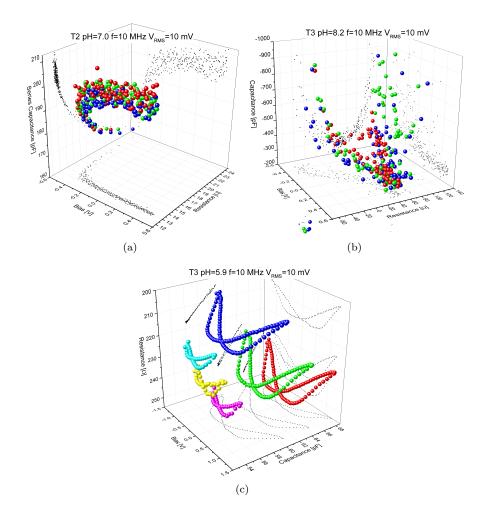
9

Figure 6: 3D plots showing series resistance and capacitance versus bias at 10 MHz and fixed signal amplitude (10 mV), for sample (a) T2 pH 7.0, (b) T3 pH 8.2, and (c) T3 pH 5.9. Colour code identifying measures on different droplet samples. Black dots on coordinated planes are to help the reader in extracting binary dependencies (capacitance vs bias, resistance vs bias, and capacitance vs resistance).

10

interesting results are found in the basic form of T3, where experimental points describe a saddle surface, resulting in two branches that during the sweep have similar negative capacitance but resistance of opposite sign, opening potential applications as voltage controlled gain passive device or voltage controlled negative capacitors [26, 27]. The most peculiar behaviour is found in the acid condition for T3, where a butterfly chaotic response is recorded. Such butterfly diagrams in impedance are associated with ferroelectric response [28], therefore this is the fingerprint of electrical polarisability of tectomer molecules excited by the signal oscillation at 10 MHz. Some cycles acquired in the 0.5 V range have shown a stable slightly asymmetric butterfly response, at different impedance values (chaotic), while other cycles acquired in the 1.2 V extended range have shown a stable chaotic symmetric butterfly response (see in particular the coordinated bottom plane capacitance vs bias).

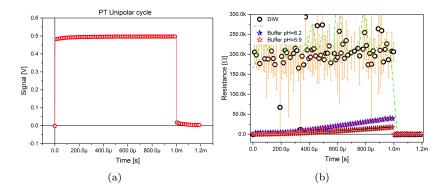*3.3. Pulse Train measurements*

(a)

(b)

Figure 7: Unipolar pulse submitted to samples in (a) the PT characterization and (b) DIW and buffer solutions response to the same (dashed line: adjacent averaging over 50 points, for DIW sample only). 1 point of every 50 is shown for clarity.

The pulse shape of the Pulse Train (PT) is presented in Fig. 7. DIW response to a unipolar pulse is shown, evidencing a noisy and rather flat resistance, with no distortion induced by high order harmonics; the rest resistance value is about -950 Ω, that we may take as reference for further considerations on other materials. Conversely, the buffer solutions confirm their highly conductive state and a linear response to the step function given as input.

Shown in figures 8(a)–8(c) is a comparison between the unipolar pulse response of tectomers at neutral pH. The ultimate resistance achieved at the end of the positive waveform is inversely proportional to the number of legs of the tectomer. T4 shows a peculiar response, with a more stable profile and a much smaller deviation. The effect of pH is shown in Figs. 8(d)–8(e): both the acid and basic condition result in a linear response with very low deviation, at least in the first portion of the waveform, while their pure buffers show a clear distortion in the first portion of the waveform. Two properties are very different: the ultimate
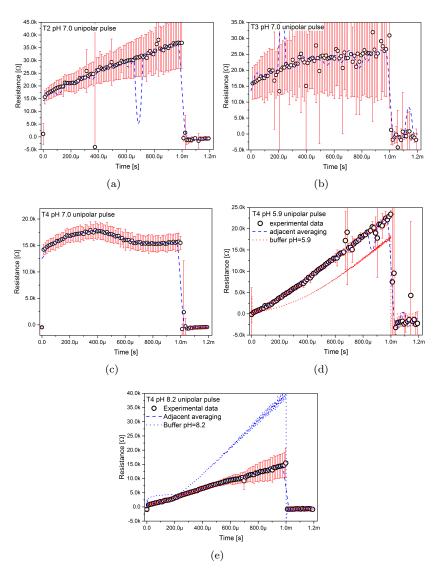
11

Figure 8: PT unipolar pulse submitted to (a) T2, (b) T3, and (c) T4 in neutral condition; and (d) T4 in pH=5.9 compared to its buffer solution, and (e) T4 in pH=8.2 compared to its buffer solution. Only 1 point every 10 shown for clarity. Average over 10 experimental curves (black open dots, red bars: standard deviation) superimposed to a smoothing over 50 adjacent points (dashed blue).

12

resistance in case of acid condition is slightly higher than that of the pure buffer (Fig. 8(d)) , while in case of basic condition is much lower (Fig. 8(e)). We might observe that the basic condition, where self-assembly of tectomer molecules is obtained, provides a more responsive behaviour to electrical stimuli in the high frequency range, while the acid condition, where tectomer molecules are in the amorphous state, is less responsive and shows higher impedance. Also the noise pattern is different: the sample kept at pH=5.9 features random noise (Fig. 8(d)), while the sample at pH=8.2 features a slightly chaotic profile that in turn produces a high standard deviation over averaging (Fig. 8(e)).
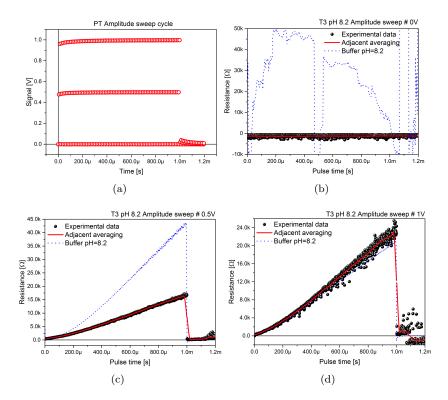

Figure 9: (a) Amplitude sweep pulses submitted to samples in the PT characterization, time-shifted to appear in the same graph. 1 point every 20 shown for clarity. (b) Amplitude sweep response of sample T3 at pH=8.2 to the amplitude sweeps at 0 V, (c) 0.5 V, and (d) 1.0 V; compared with its buffer solution. All experimental points are shown.

In another operation mode, the amplitude sweep cycle, the sample is submitted to a train of pulses of growing amplitude, repeated 50 times. As shown in Fig. 9, we set three steps at 0, 0.5 and 1.0 V, each lasting 1 ms, and separated from the others by 4 ms of idle time at zero bias. Ten measurements are acquired as usual to follow any chaotic behaviour. Again in Fig. 9 sample T3 at pH=8.2 has been shown, separating the three amplitude sweeps for clarity in different panels. We might observe that, while an increased polarizability and lower

13

impedance response with respect to the pure buffer is seen at 0 and 0.5 V, when signal amplitude increases to 1.0 V the tectomers in basic solution show a slightly higher impedance. This means that high amplitude signals are able to interfere with the self-assembled crystalline structure and amorphise it.

3.4. Comparison

To clarify the differences between tectomers and pH conditions, relevant data from the plots of both unipolar pulses and amplitude sweeps have been extracted and presented in Tab. 1. By comparing the slew rate (resistance increase speed, within the period of the pulse) extrapolated from the unipolar pulse measures and the amplitude sweep ones, we see a rather good agreement. The asymptotic resistance values at zero bias are nevertheless very different in the two techniques, and they show a positive correlation with the number of tails of the tectomer: the higher the number, the higher the absolute value of asymptotic terms, at any pH values. The slew rate shows on the contrary an inverse correlation with the number of tails, which holds in neutral conditions: the higher the number, the slower the resistance growth rate. When the solution is acidic or basic, the fastest response is found either for T3 or T4. Interestingly, the highest slew rates are generally found for the intermediate potential (0.5 V) in the amplitude sweep condition.

4. Discussion: Towards zettascale computing

While exascale (1EFlops = 10^{18} operations/s) computing systems are expected to be deployed in the first years of 2020, zettascale computing systems should reach their milestone in 2035 [16]. As for now, with the end of the Moore's scaling era approaching and the physical constraints related to thermal dissipation issues, Johnson noise and leakage, there are no clear routes towards such high performance computers. Rather, a number of developments both at hardware and at software level should be achieved simultaneously to concur to such milestone. On the other hand, liquid systems offer tangible advantages, especially in terms of dissipated power against computing operation.

Let's define the physical scenario: a 1 litre sphere of tectomer solution (radius 62.035 mm) that is used to store information. The size of one single bit of information is physically limited by the size of the quanta, in our case in the range of 50 nm [21], and by the size of the smallest physical feature we are able to "write" in the liquid medium. Electromagnetic waves are easily diffracted and focused, while electric signals require routing and necessarily involve more expensive technologies to create electrode patterns. An optical signal, in other words a spatial and temporal distribution of intensity patterns that can affect locally the pH of the solution [29] and therefore the aggregation state of the solvated tectomers, will therefore be able to write bits of information. Optical wavelengths such as 532 nm make it possible to work with inexpensive coherent light sources and extremely powerful focusing elements based, for instance, on metamaterials; where the smallest volume affected by light could be around

14

Table 1: Data extrapolated from the PT measurements, the first three columns in the unipolar pulse mode, the last five columns in the amplitude sweep mode. The asymptotic resistances R∞ are computed from the 50 points adjacent averaging smoothed curves, the slew rates are the slope of a linear fit to the smoothed curves, whose R2 is also reported.

Sample	R∞@uni [Ω]	Slew rate [$\Omega\,s^{-1}$]×10^6	R2 [-]	R∞@ampl.sw [Ω]	Slew rate @ 0.5 V [$\Omega\,s^{-1}$]×10^7	R2 [-]	Slew rate @ 1.0 V [$\Omega\,s^{-1}$]×10^7	R2 [-]
T2 pH=7.0	-1095	(2.44Ω0.03)×10	0.95151	178168	(3.391±0.003)×10	0.99951	(3.410±0.003)×10	0.99946
T3 pH=7.0	-81	(2.0±0.3)×10	0.17399	235505	(3.54±0.04)×10	0.88076	(2.30±0.02)×10	0.96
T4 pH=7.0	-436	(1.27±0.04)	0.88628	352601	(3.61±0.02)×10	0.89996	(1.28±0.05)×10	0.96
T2 pH=5.9	-137	(2.00±0.01)×10	0.99472	-739	(2.357±0.008)×10	0.99591	(2.165±0.002)×10	0.99975
T3 pH=5.9	-1070	(4.57±0.01)×10	0.99747	-991	(3.41±0.02)×10	0.98763	(3.1±0.1)×10	0.67551
T4 pH=5.9	-1215	(2.352±0.004)×10	0.99893	-2092	(2.962±0.006)×10	0.99725	(2.653±0.007)×10	0.99452
T2 pH=8.2	-179	(2.850±0.003)×10	0.99933	-908	(2.842±0.003)×10	0.99929	(2.341±0.002)×10	0.99928
T3 pH=8.2	-1145	(2.224±0.003)×10	0.9994	-1322	(1.866±0.002)×10	0.9993	(2.641±0.002)×10	0.99963
T4 pH=8.2	-725	(1.543±0.001)×10	0.99966	-2096	(2.96±0.03)×10	0.94693	(3.05±0.04)×10	0.92256

375×375 nm^2 [30]. Considering a reasonable pitch between intensity nodes (1,000 nm) and concentric shells carrying information within the solution sphere volume, one may easily verify that the total amount of bits stored in a 1 litre sphere is over 10 Tbits. The fastest optical modulator available with current technology is able to create and refresh a diffraction grating with a frequency of 5 kHz, making it possible to theoretically store data with a rate of $2.5\,\mathrm{Tbit\,s^{-1}}$ [31] using an optical power in the order of $0.1\,\mathrm{mW\,m^{-2}}$. If we imagine to work on a plane and optically write data on the 1 litre sphere with gratings positioned at $-x$, $+x$, $-y$ and $+y$, our speed becomes $10\,\mathrm{Tbit\,s^{-1}}$ and our overall power consumption lower than 100 mW. Now data is transferred to the whole volume of a 1 litre sphere, and we are ready to perform computations by submitting spherical electromagnetic waves to this densely packed grating. Waves will collect spatial information and produce a scattering/absorption pattern that represents our computational result. This sort of computation requires a mathematically different framework, based on holography [32]. One single holographic operation is not equivalent to a floating point operation, as it involves the physics of continuum [33]. With a sufficient high signal to noise ratio, one holographic operation could be the equivalent of 1,000 floating point 64 bit-based operations. Therefore our energy consumption is 200 mW/10 PFlops or 20 kW/ZFlops. This result opens tremendous possibilities in terms of distributed edge computing, energy saving and pervasivity of big data computation.

5. Summary

It was demonstrated that tectomers are versatile nanomaterials with non-trivial electronic properties which are, at least partly, determined by the pH of the medium and the number of olygoglycine tails. Direct current-voltage (I-V) cycles measured on 4-tailed tectomers at neutral pH show increase of the maximum current flowing with each cycle, more likely due to re-ordering of tectomers and formation of layers with increased conductivity. In some samples, oscillations of I-V curve have been observed, which might indicate that in some parts of the droplet assembly and disassembly processes co-exist. Behaviour of the tectomers during I-V sweep is determined by the pH of the solution and the number of tails (2, 3, or 4). The I-V curves show that 2-tailed species in acidic environment (amorphous case) can be used as resistive switching devices.

It was found that it is possible to distinguish between the different tectomers and/or the pH of their solution by measuring their impedance in the range between 1 kHz and 1 MHz. Additionally, 3-tailed tectomers could be used as voltage controlled gain passive devices in the 10 MHz region, because the series resistance-capacitance-bias locus shows similar negative capacitances but opposite sign resistances. Interestingly, 3-tailed tectomers show ferroelectric-like response, under acidic solution (amorphous case), with a clear butterfly diagram in the plane series-capacitance vs bias.

Pulse train comparative analysis showed that the acidic environment (amorphous structure) provides a higher impedance with respect to the pure buffer, while the basic environment (self-assembled crystalline structure) provides a

lower impedance, until 0.5 V of signal amplitude. It was also observed that increasing signal amplitude up to 1.0 V breaks the self-assembled ordered state, in the basic environment, and thereby increases the impedance. It was observed that asymptotic resistance of tectomers is proportional to the number of tails, while the slew rate is inversely proportional to the number of tails.

This represents the first step towards the use of tectomers as intrinsic electrical components, furthering low-power high-speed computing.

Acknowledgements

References

[1] A. Chiolerio, M. Quadrelli. *Advanced Science* **2017**, *4*, 7 1700036.

[2] A. Chiolerio, M. B. Quadrelli. *Energy Technol.* **2019**, *7*, 5 1800580.

[3] A. Chiolerio, I. Roppolo, K. Bejtka, A. Asvarov, C. F. Pirri. *RSC Advances* **2016**, *6* 56661.

[4] T. C. Draper, C. Fullarton, N. Phillips, B. P. de Lacy Costello, A. Adamatzky. *Mater. Today* **2017**, *20*, 10 561.

[5] J. Čejková, T. Banno, M. M. Hanczyc, F. Štěpánek. *Artificial life* **2017**, *23*, 4 528.

[6] A. Adamatzky, B. De Lacy Costello, C. Melhuish, N. Ratcliffe. *AISB Quarterly* **2003**, *112*, 5.

[7] A. Sadeghi, L. Beccai, B. Mazzolai. In *Intelligent Robots and Systems (IROS), 2012 IEEE/RSJ International Conference on.* IEEE, **2012** 4237–4242.

[8] A. Hirono, T. Toyota, K. Asakura, T. Banno. *Langmuir* **2018**, *34*, 26 7821.

[9] B. L. Stoimenov, J. Rossiter, T. Mukai. In *Electroactive Polymer Actuators and Devices (EAPAD) 2009*, volume 7287. International Society for Optics and Photonics, **2009** 72872B.

[10] S.-W. Yeom, I.-K. Oh. *Smart materials and structures* **2009**, *18*, 8 085002.

[11] J. Zhang, Y. Yao, L. Sheng, J. Liu. *Advanced Materials* **2015**, *27*, 16 2648.

[12] C. B. Eaker, M. D. Dickey. *Applied Physics Reviews* **2016**, *3*, 3 031103.

[13] A. Adamatzky. *Philos. Trans. R. Soc. B Biol. Sci.* **2019**, *374*, 1774 20180372.

[14] C. Fullarton, T. C. Draper, N. Phillips, B. P. J. de Lacy Costello, A. Adamatzky. *J. Phys. Mater.* **2019**, *2*, 1 015005.

[15] K. H. Pribram. *Brain and perception: Holonomy and structure in figural processing.* Psychology Press, New York, **2013**.

[16] X.-k. Liao, C.-q. Yang, J.-w. Li, Y. Yuan, M.-c. Lai, L.-b. Huang, P.-j. Lu, J.-b. Fang, J. Ren, J. Shen. *Frontiers of Information Technology & Electronic Engineering* **2018**, *19*, 10 1236.

[17] S. V. Tsygankova, A. A. Chinarev, A. B. Tuzikov, N. Severin, A. A. Kalachev, J. P. Rabe, A. S. Gambaryan, N. V. Bovin. *Beilstein journal of organic chemistry* **2014**, *10* 1372.

[18] A. B. Tuzikov, A. A. Chinarev, A. S. Gambaryan, V. A. Oleinikov, D. V. Klinov, N. B. Matsko, V. A. Kadykov, M. A. Ermishov, I. V. Demin, V. V. Demin, P. D. Rye, N. V. Bovin. *ChemBioChem* **2003**, *4*, 2-3 147.

[19] I. Gorokhova, A. Chinarev, A. Tuzikov, S. Tsygankova, N. Bovin. *Russian Journal of Bioorganic Chemistry* **2006**, *32*, 5 420.

[20] V. Bovin, A. Tuzikov, A. Chinariov. *Rossijskije Nanotekhnologii* **2008**, *3*, 5-6 98.

[21] A. Y. Gyurova, A. Michna, L. Nikolov, E. Mileva. *Colloids and Surfaces A: Physicochemical and Engineering Aspects* **2017**, *519* 106.

[22] I. Jurewicz, R. Garriga, M. J. Large, J. Burn, N. Bardi, A. A. K. King, E. G. Velliou, J. F. Watts, S. J. Hinder, E. Muñoz, A. B. Dalton. *ACS Appl. Nano Mater.* **2018**, *1*, 8 3903.

[23] R. Garriga, I. Jurewicz, E. Romero, C. Jarne, V. L. Cebolla, A. B. Dalton, E. Muñoz. *ACS applied materials & interfaces* **2016**, *8*, 3 1913.

[24] K. Rajan, K. Bejtka, S. Bocchini, D. Perrone, A. Chiappone, I. Roppolo, C. F. Pirri, C. Ricciardi, A. Chiolerio. *J. Mater. Chem. C* **2017**, *5*, 25 6144.

[25] N. Elgrishi, K. J. Rountree, B. D. McCarthy, E. S. Rountree, T. T. Eisenhart, J. L. Dempsey. *J. Chem. Educ.* **2018**, *95*, 2 197.

[26] M. Laurenti, A. Verna, A. Chiolerio. *ACS Applied Materials and Interfaces* **2015**, *7* 24470.

[27] A. Chiolerio, S. Porro, S. Bocchini. *Advanced Electronic Materials* **2016**, *2* 1500312.

[28] A. I. Khan, D. Bhowmik, P. Yu, S. J. Kim, X. Pan, R. Ramesh, S. Salahuddin. *Applied Physics Letters* **2011**, *99* 113501.

[29] B. Ouyang, K. Zhang, Y. Yang. *iScience* **2018**, *1* 16.

[30] M. Khorasaninejad, W. T. Chen, R. C. Devlin, J. Oh, A. Y. Zhu, F. Capasso. *Science* **2016**, *352*, 6290 1190.

[31] A. Srivastava, W. Hu, V. Chigrinov, A. Kiselev, Y.-Q. Lu. *Applied Physics Letters* **2012**, *101* 031112.

405 [32] K. Preston. *Pattern Recognit.* **1973**, *5*, 1 37.

[33] M. L. Yevick. *Pattern Recognit.* **1975**, *7*, 4 197.